

# An experimental investigation on forced convection heat transfer performance in micro tubes by the method of liquid crystal thermography

Ting-Yu Lin, Chien-Yuh Yang\*

*Department of Mechanical Engineering, Institute of Energy Engineering, National Central University, Chung-Li 32054, Taiwan*

Received 6 November 2006; received in revised form 1 March 2007

Available online 8 June 2007

## Abstract

This study proposed a non-contacted liquid crystal thermography (LCT) method for micro tube surface temperature measurement. It avoids the thermal shunt error caused while using the direct contact thermocouples. Two stainless steel tubes with inside diameter of 123  $\mu\text{m}$  and 962  $\mu\text{m}$  were tested. The test results agree very well with those predicted by the conventional correlations. It successfully extends the validity of conventional single-phase heat transfer correlations to the tube with inside diameter of 123  $\mu\text{m}$ . This method can be further applied for measuring smaller tube surface temperature that the thermal shunt may be more significant by using direct contact temperature measurements methods.

© 2007 Elsevier Ltd. All rights reserved.

*Keywords:* Liquid crystal thermography (LCT); Micro tube; Forced convection heat transfer; Thermal shunt

## 1. Introduction

The study on heat transfer performance in micro tubes has become more important due to the rapid growth of the application for high heat flux electronic devices cooling. However, definitive information on heat transfer coefficient of such small channels is not available in the published literatures. The traditional forced convection heat transfer correlations were derived from tubes with diameter much larger than those used in micro-channels. They have not been verified to work well for predicting the heat transfer coefficient inside small hydraulic diameter tubes. Several researches dealing with the single-phase forced convection heat transfer in micro tubes have been published in the past years. Most of their tests results are significantly departed from those of the traditional forced convection heat transfer coefficients in larger tubes. Guo and Li [1] proposed that the measurement accuracy is one of the most impor-

tant factors that may cause this discrepancy. Since the diameter of the sensor for measuring micro tubes surface temperature is comparable to the size of the micro tubes, the tube surface temperature cannot be accurately measured due to the effect of sensor wire thermal shunt. A non-contacted temperature measurement method must be developed for precisely measuring the micro tube surface temperature without thermal shunt effect.

Attributed to the dramatic progressive of image processing technologies, liquid crystal thermography (LCT) has been widely used for qualitatively and quantitatively surface temperature measurement in the past decade. The surface which to be measured was coated with thermochromic liquid crystal (TLC). By illuminating white light, TLC reacts to change color continuously by changing its temperature. Color of liquid crystal at working range may be defined as a property of light and represented by three characteristics, i.e. hue, saturation and intensity. Camci et al. [2] indicated that a direct relation between the local temperature and the locally measured hue value could be experimentally established. The change of hue value with

\* Corresponding author. Tel.: +886 3 4267347; fax: +886 3 4254501.  
E-mail address: [cyyang@ncu.edu.tw](mailto:cyyang@ncu.edu.tw) (C.-Y. Yang).

## Nomenclature

$A$	heat transfer area ( $\text{m}^2$ )	$Nu_d$	Nusselt number (dimensionless)
$A_c$	tube cross section area ( $\text{m}^2$ )	$q$	heat transfer rate (W)
$c_p$	specific heat (J/kg K)	$Re_d$	Reynolds number (dimensionless)
$d_i$	tube inside diameter (m)	$T_i$	inlet water temperature ( $^{\circ}\text{C}$ )
$f$	friction factor (dimensionless)	$T_x$	local water temperature ( $^{\circ}\text{C}$ )
$G$	mass velocity ( $\text{kg}/\text{m}^2 \text{ s}$ )	$T_{wx}$	local tube inside wall temperature ( $^{\circ}\text{C}$ )
$h$	heat transfer coefficient ( $\text{W}/\text{m}^2 \text{ }^{\circ}\text{C}$ )	TLC	thermochromic liquid crystal
$H$	hue value (dimensionless)	$x$	axial position of tubes (m)
$k$	water conductivity ( $\text{W}/\text{m }^{\circ}\text{C}$ )		
$L$	tube heating length (m)		
LCT	liquid crystal thermography		
$\dot{m}$	mass flow rate (kg/s)		
		<i>Greek symbol</i>	
		$\mu$	viscosity ( $\text{N}/\text{m}^2 \text{ s}$ )

temperature is reversible and repeatable. Their data showed that the variation of local light intensity did not strongly alter the hue value and the influence of illumination angle below  $40^{\circ}$  is negligible. The present study applies the above stated non-contacted liquid crystal thermography method for micro tube surface temperature measurement. It avoids the thermal shunt error caused while using the direct contact thermocouples.

## 2. Experimental method

### 2.1. Tubes dimensions

Two smooth stainless steel tubes with inside diameter of  $123 \mu\text{m}$  and  $962 \mu\text{m}$  were tested in this study. The tubes diameters were measured from the enlarged photographs taken by scanning electron microscope (SEM) and optical

microscope (OM) for  $123 \mu\text{m}$  and  $962 \mu\text{m}$  tubes, respectively. Fig. 1 shows the sample enlarged photographs of the cross section view of the tubes. For reducing the measurement uncertainties, several tubes were bundled together, cut and polished to have smooth cross section surface. For each size of tube, each tube was measured and all tubes' diameters were averaged to obtain the average tube diameter. Table 1 gives the detail dimensions of these tubes. The surface roughness for both tubes was also measured as  $1.4 \mu\text{m}$ .

### 2.2. Experimental system setup

Fig. 2 shows the schematic diagrams of the test facilities. A pressure vessel connected to high-pressure nitrogen was used to push the water through test tubes. The inlet water temperature was measured by a resistance temperature

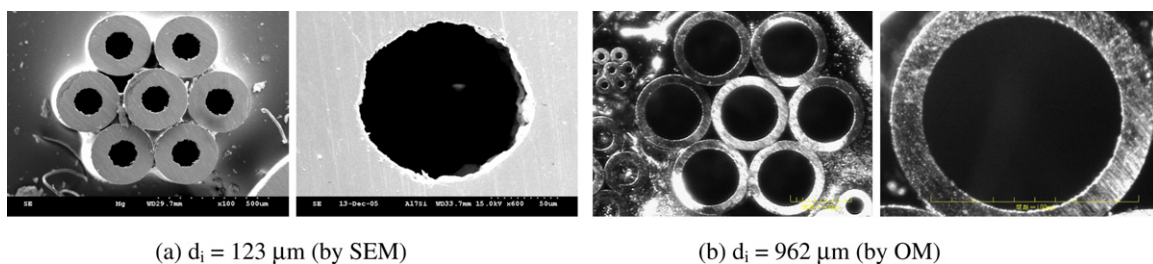


Fig. 1. Enlarged photographs of the micro tubes.

Table 1  
Detail dimensions of the tubes tested

Tube notation	Tube length (mm)	Number of tubes measured	Average outside diameter, $d_o$ ( $\mu\text{m}$ )	Average inside diameter, $d_i$ ( $\mu\text{m}$ )	Standard deviation ( $\mu\text{m}$ )	Wall temperature measuring position (mm)	Heating length, $L$ (mm)
$123 \mu\text{m}$ (L)	140	15	250	123	1.00	75	120
$123 \mu\text{m}$ (S)	64					29	34
$962 \mu\text{m}$	356	14	1260	962	1.28	287	327

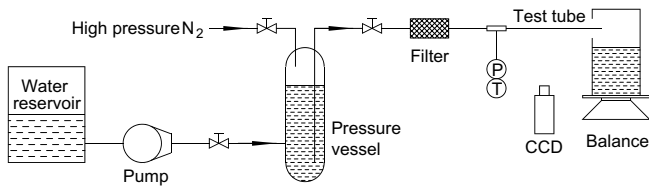


Fig. 2. Schematic diagrams of the test facilities.

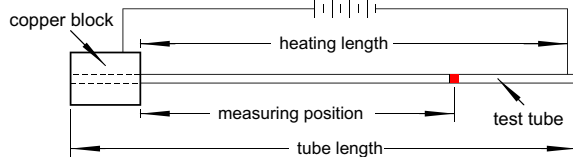


Fig. 3. Detail dimensions of the test section.

detector (RTD). DC power was clapped on both ends of the test tube to heat the tube surface. The flow rate was measured by weighting the water collected in the container on a programmable electronic microbalance. The detail of the test section is shown in Fig. 3. Test tube was soldered in a copper block which to fit with the inlet piping. The heating length and temperature measuring position shown in Fig. 3 for each tube are also listed in Table 1. The measuring position was designed to be longer than the maximum theoretical laminar flow entrance length. However, because of the test space limitation, the length of the 962  $\mu\text{m}$  tube is slightly shorter than that entrance length.

### 2.3. LCT temperature measurement

Four TLCs with 5  $^{\circ}\text{C}$  bandwidth from 28 to 33, 33 to 38, 38 to 43 and 45 to 50  $^{\circ}\text{C}$  were used in the present study for increasing the accuracy of tube wall temperature measurement. Those LCTs were made by Hallcrest, Inc., USA, with product numbers of BM/R28C5W/C17-10, BM/R33C5W/C17-10, BM/R38C5W/C17-10 and BM/R45C5W/C17-10. The diameters of the encapsulated TLCs are ranging from 5 to 15  $\mu\text{m}$ . The TLCs was painted on the tested tubes surface with a thickness of approximately 30  $\mu\text{m}$ . A black paint was also painted under the TLCs as the background for improving the color resolution by absorbing un-reflected light.

The image processing system included a single charge-coupled-device (CCD) color video camera, a frame grabber card and a personal computer. The CCD camera with resolution of  $640 \times 480$  pixels was set on a slipping rail parallel to the micro tube tested. A 1000 mm ruler was attached near the slipping rail to measure the displacement of CCD camera. The actual size on the tube surface related to one pixel of the CCD image is about 13–14  $\mu\text{m}$  in the present study. The moving rail mechanism was designed to allow the CCD to move and take photographs quickly without adjusting the depth of field again. The lighting source was also installed on the slipping rail and moved with the

CCD camera. A common fluorescent tube was used for illumination as suggested by Ireland et al. [3]. Since the proportion of the radiation in the infrared region of the fluorescent tube spectrum is low, it will not cause significant heating for the test surface. Since the lighting condition may influence the color of the liquid crystal, any uncontrollable light should not be allowed while test is undergoing. Black drapes were installed around the entire experimental system to block out the external light and ensure that the hue values of TLC were not influenced. The images captured by the CCD were recorded by the personal computer and could also be displayed on the monitor. The frame grabber card digitizes the CCD images and converts the standard RGB (red, green and blue) signals to HSI (hue, saturation and intensity) signals with a value range from 0 to 255.

The relation between the hue value and temperature was calibrated by putting the test section in a thermostat box which was designed to maintain the entire test section at constant and uniform temperature condition. Electrical heating wires were attached on the inside surfaces of the box. The temperature inside the thermostat box can be adjusted by setting the input power on the heating wire. Seven T-type thermocouples were evenly placed on the test tube surface to measure its temperature distribution. The liquid crystal thermograph and temperature measured by thermocouples were recorded simultaneously. Fig. 4 shows the temperature distribution inside the thermostat box at different temperature setting conditions. The temperature uniformity inside the box is within  $\pm 0.1$   $^{\circ}\text{C}$  at different temperature setting conditions. For reducing noise, the hue value was averaged within an area of 10 pixels (radial)  $\times$  100 pixels (axial) for the 962  $\mu\text{m}$  tube and 5 pixels (radial)  $\times$  50 pixels (axial) for the 123  $\mu\text{m}$  tube. The hue value to temperature calibration results for each temperature range TLCs on 123  $\mu\text{m}$  tube are shown in Fig. 5.

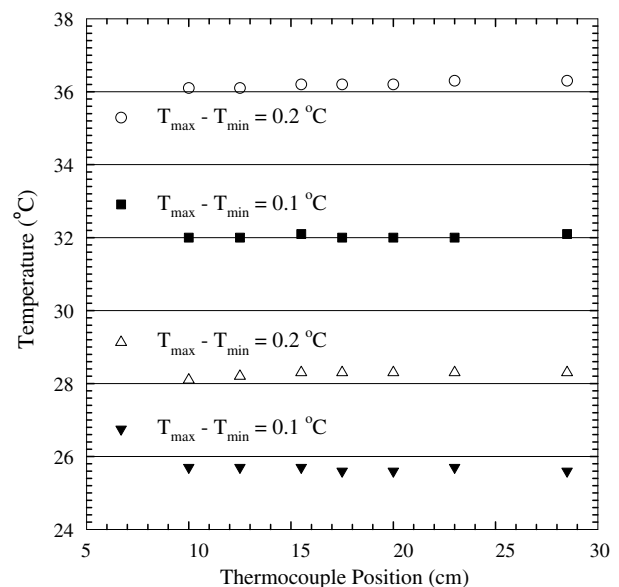


Fig. 4. Temperature distribution inside the thermostat box.

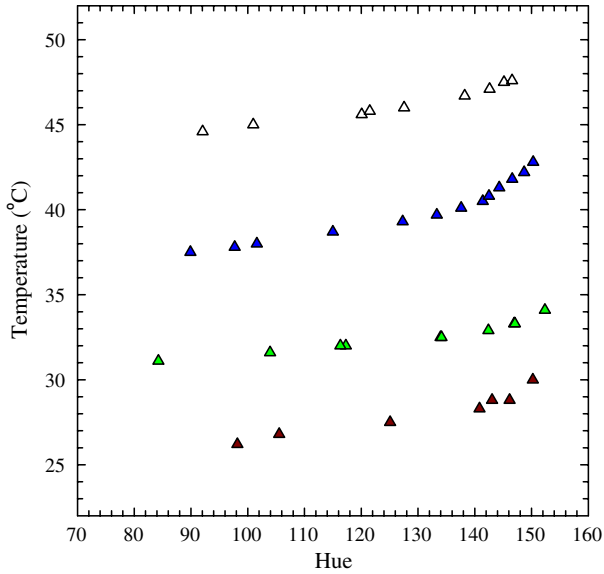


Fig. 5. Temperatures versus hue values calibration curves for each temperature range TLCs on 123  $\mu\text{m}$  tube.

The figure shows that the sensitivity of hue value relative to temperature variation is approximately 20  $1/^\circ\text{C}$  for hue value lower than 140 but it is only 5.0  $1/^\circ\text{C}$  for hue value higher than 140. Therefore, the heating power was adjusted to keep the surface TLC hue values within the range from 80 to 140 to minimize the temperature measurement uncertainty during the test for different flow rate in the present study.

#### 2.4. Data reduction and uncertainty analysis

The heat transfer rate  $q$  was measured from the DC power input deducted by tube outer surface heat loss and it equals to the water flow enthalpy change. The heat loss from the tube outer surface was determined by a separate experiment without water flow inside it. The test tube was heated to keep at a uniform temperature which is the same as the measuring point temperature of the heat transfer test. The heating rate was recorded. Since during the heat transfer test, the tube surface temperature varied near linearly from the inlet water temperature to the measuring point temperature. The heat loss can be estimated as the half of the heating rate recorded in the heat loss test times the fraction of measuring position length to the heating length. The estimated heat loss is less than 4% and 1% of the total heat input for 123  $\mu\text{m}$  tube and 962  $\mu\text{m}$  tube, respectively.

Since the electrical power was added uniformly on the tube surface, the local water temperature  $T_x$  at position  $x$  from the beginning of the heating point can be estimated from the following energy balance:

$$q \frac{x}{L} = \dot{m} c_p (T_x - T_i) \quad (1)$$

where  $\dot{m}$  is the water flow rate,  $L$  is the total heating tube length and  $T_i$  is the water inlet temperature.

The local heat transfer coefficient  $h$  can be calculated from the Newton's Law of cooling as

$$h = \frac{q}{A(T_{\text{wx}} - T_x)} \quad (2)$$

where  $A = \pi d_i L$  is the heat transfer area and  $T_{\text{wx}}$  is the local tube inside surface temperature that can be derived from the LCT measured outside surface temperature by the method of one-dimensional heat conduction analysis. The relative Reynolds number and Nusselt number are defined as

$$Re_d = \frac{G d_i}{\mu} \quad \text{and} \quad Nu_d = \frac{h d_i}{k} \quad (3)$$

where  $G (= \dot{m}/A_c)$  is the water flow mass flux through the tube with cross section area  $A_c$ .

Since the tubes are small, the tube wall thickness is comparable with the inside diameter, the heat conduction in the wall along axis direction may be important. This axial conduction was estimated by the method of Maranzana et al. [4]. The results show that the ratio of axial conduction to the tube inside convection is less than  $8.9 \times 10^{-5}$  and  $1.1 \times 10^{-5}$  for 123  $\mu\text{m}$  tube and 962  $\mu\text{m}$  tube, respectively, and thus can be neglected.

The uncertainty of the temperature value for a single pixel can be obtained by using the polynomial on the hue value fitting curve of this pixel which presented by Hay and Hollingsworth [5]. The uncertainty  $\delta T$  is calculated as

$$\delta t = \left[ (2\text{SEE})^2 + \left( \frac{dT}{dH} \delta H \right)^2 \right]^{\frac{1}{2}} \quad (4)$$

where  $dT/dH$  is the slope of the hue value fitting curve and  $\delta H$  is the standard deviation of average hue obtained from each pixel of the data region. The standard estimate error (SEE) is defined as

$$\text{SEE} = \left[ \frac{\sum_{i=1}^n [T_i(H) - T_{\text{fit},i}(H)]^2}{n - j - 1} \right]^{\frac{1}{2}} \quad (5)$$

where  $n$  is the number of data point,  $j$  is the order of the curve fit,  $T_i(H)$  is the measured temperature relative to the hue value  $H$  and  $T_{\text{fit},i}$  is the temperature calculated from the temperature–hue fitting curve. The standard deviation for the calibrated temperature–hue curve was evalu-

Table 2  
Uncertainties of the experimental apparatus and derived parameters

Apparatus	Uncertainties	Calibrated range
RTD	$\pm 0.1$ $^\circ\text{C}$	10–70 $^\circ\text{C}$
T-type thermocouple	$\pm 0.2$ $^\circ\text{C}$	0–70 $^\circ\text{C}$
Balance (A)	$\pm 0.015$ g	4200 g
Balance (B)	$\pm 0.005$ g	850 g
<i>Derived parameters</i>		
$Re_d$	0.4–3.9%	
$Nu_d$	2.0–12%	

ated within  $\pm 0.4\text{ }^\circ\text{C}$ . The experimental apparatus and derived parameters uncertainties are listed in Table 2.

### 3. Results and discussion

#### 3.1. Viewing angle effect

Due to the viewing angle effect on a circular tube surface, the hue value on the upper and lower region of the tube surface is not the same as that on the central region even though they are at the same temperature. Chan et al. [6] investigated the influence of viewing angle on measuring the temperature by liquid crystal thermography. Their data showed that the influence of viewing angle was not significant while it is under  $18^\circ$ . Camci et al. [2] indicated that the relationship between the hue values and temperature would not change even if the intensity has a difference of up to 25%. Due to the shape of test tube surface in the present study, the intensity of TLC is lower in the upper and lower regions as shown in Fig. 6. However, the intensity in the middle region with  $Y$  direction pixels from  $-3$  to  $3$  varies from 168.2 to 172.9 for  $962\text{ }\mu\text{m}$  tube and from 122.6 to 136.3 for  $123\text{ }\mu\text{m}$  tube, which is much lower than the allowable range that proposed by Camci et al. [2]. Fig. 7 shows the respective vertical hue values variation of TLC on micro tube surface. The hue values varies from 111.9 to 114.2 and 121.1 to 124.8 for  $962\text{ }\mu\text{m}$  and  $123\text{ }\mu\text{m}$  tubes, respectively, within  $\pm 3$  pixels observation region from the central region. Referring to the TLCs calibration results shown in Fig. 5, the viewing angle effect on hue value caused approximately  $0.15\text{ }^\circ\text{C}$  temperature measurement uncertainties.

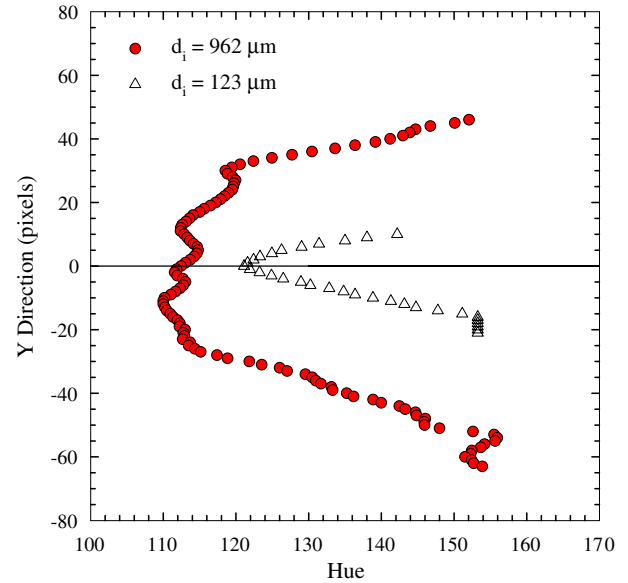


Fig. 7. Effect of viewing angle for TLC hue values on micro tube surface.

#### 3.2. Friction factors

Fig. 8 shows the friction factors of water flows in the tubes tested. They agree very well with the conventional Blasius ( $f = 0.079Re_d^{-0.25}$ ) and Poiseuille ( $f = 16/Re_d$ ) equations in turbulent and laminar flow regime, respectively. Yang et al. [7] measured the friction factors of water flow in tubes with diameter ranging from 0.5 to 4.0 mm. They found that there is no significant discrepancy for water flow in these range tubes in comparing with larger tubes. The present study extends the test tube size to the smaller tube with inside diameter of  $123\text{ }\mu\text{m}$ . It is clear that there is no significant physical difference for water flows in

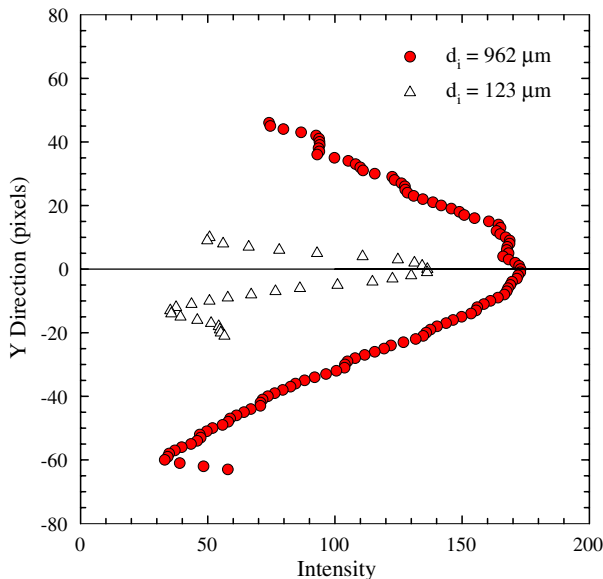


Fig. 6. Effect of viewing angle for TLC intensity values on micro tube surface.

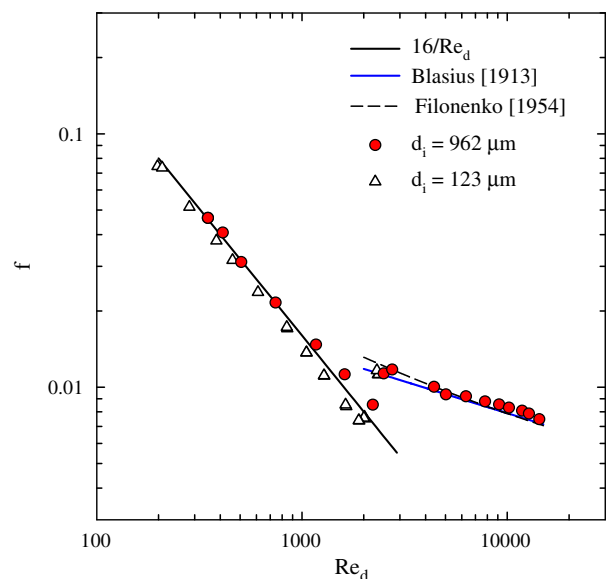


Fig. 8. Friction factors for water flow in 123 and  $962\text{ }\mu\text{m}$  tubes.



tubes larger than 0.1 mm. The conventional theories are applicable for flow in this size range.

3.3. Heat transfer coefficient

A sample photograph and the analyzed tube surface temperature distribution map of 28–33 °C TLC for water flow heated in a 962 μm inside diameter tube are shown in Fig. 9. A calibrated temperature color bar was also attached for reference. The temperature increases from the left hand side to the right hand side with color changes from red to blue, respectively. While out of the designated temperature range, the TLC remains transparent and the black background color was shown on the photograph. Fig. 10 shows the surface temperature variation along the 123 μm tube and the respective local water temperature that estimated by Eq. (1). It shows that the temperature difference between the tube surface and water increases along the water flow in the entrance region and finally approaches constant while it reaches fully developed condition.

The heat transfer test results have been reduced to the dimensionless form of the Nusselt numbers versus the Reynolds numbers and shown in Fig. 11. Some conventional heat transfer predicting curves for large tubes were also plotted for comparison. Since the driving pressure of test system provided by the high-pressure nitrogen was not high enough to reach the turbulent flow regime in 123 μm tube, a shorter tube (noted as 123 μm (S)) was also tested to verify the heat transfer performance for turbulent flow. In laminar flow regime, the measured Nusselt numbers for both 123 μm (L) and 962 μm tubes agree very well with the constant heat flux theoretical value, 4.36. However, because the length of the 123 mm (S) tube is not long enough for fully developed flow, the Nusselt numbers in high Reynolds number range flow are higher than 4.36. While the Reynolds number reaches approximately 2300, the flow regime started to transfer to turbulent. The measured turbulent Nusselt numbers for both 123 μm (S) and 962 μm tubes agree perfectly with those predicted by the Gnielinski [8] correlation.

In comparing with the previous experimental studies, the present 962 μm tube test results agree very well with those tested by Yang et al. [9] for 1.10 mm by attaching

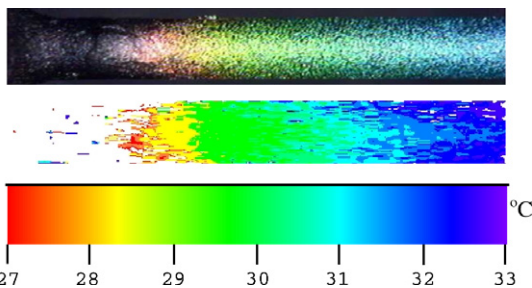


Fig. 9. Photograph and analyzed temperature distribution of LCT on the 962 μm tube.

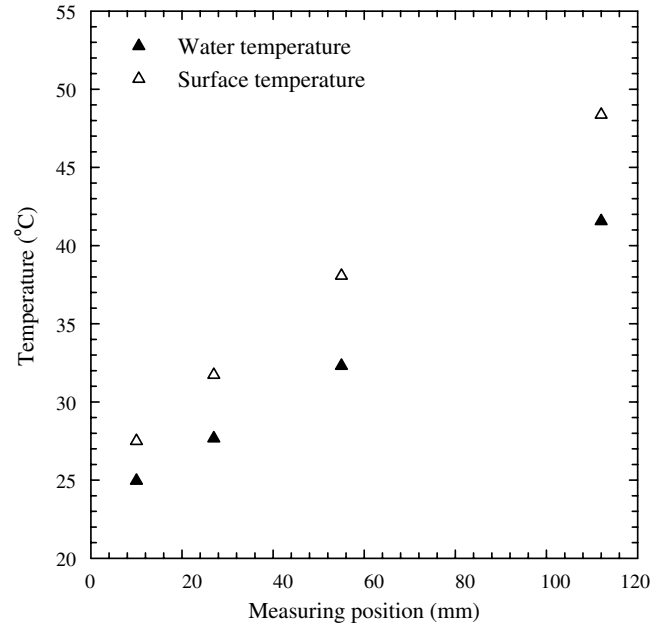


Fig. 10. Surface and water temperature variation along the heated 123 μm tube.

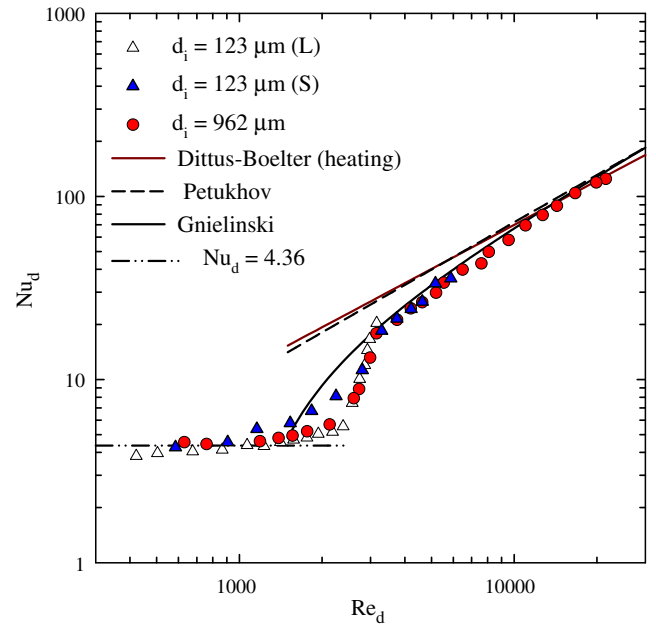


Fig. 11. Nusselt number versus Reynolds number for tubes tested.

thermocouples on the tube surface to measure the tube surface temperature. This shows the validity of using LCT method for circular surface temperature measurement.

Some experimental results on heat transfer performance in circular tubes with diameters smaller than 1.0 mm have been published in the past few years. Yu et al. [10] studied water flow in 19, 52 and 102 μm diameters tubes. Adams et al. [11] investigated turbulent single-phase forced convection of water in circular micro-channels with diameters of 0.76 and 1.09 mm. Their data showed that the Nusselt

numbers were considerably higher than would be predicted for larger tubes. The heat transfer performance increases as the channel diameter decreases and Reynolds number increases. As shown in Fig. 8, the friction factors of water flows in the present study agree very well with the conventional equations. Yu et al. [10] and Adams et al. [11] results seem suggesting that the Reynolds analogy does not hold for micro-channel flow. Yen et al. [12] measured heat transfer performance of laminar refrigerant R-123 flow in 0.3 mm diameter tube by direct attaching K-type thermocouple on the tube wall. The results are in reasonable agreement with the analytical laminar constant heat flux value ( $Nu_d = 4.36$ ). However, their data have a very high Nusselt number scattering distribution with value ranging from around 2–5. The present 123  $\mu\text{m}$  tube test results agree with those obtained by Yen et al. [12] but with much lower data scattering. It is clearly shown that the present test results can be predicted very well by the conventional correlations. This study successfully extends the validity of conventional single-phase forced convection heat transfer correlations to smaller tubes with inside diameter of 123  $\mu\text{m}$ .

From the above experimental investigation, we may find that the method of liquid crystal thermography (LCT) can be used for micro tube surface measurement with acceptable uncertainties. This method can be further applied for measuring smaller tube surface temperature that the thermal shunt effect may be significant by using direct contact temperature measurements.

#### 4. Conclusions

This study proposed a non-contacted liquid crystal thermography method for micro tube surface temperature measurement. It avoids the thermal shunt error caused while using the direct contact thermocouples. The present test results for 962  $\mu\text{m}$  tube agree very well with those by conventional test methods and prediction correlations. The 123  $\mu\text{m}$  tubes results can be predicted very well by the conventional correlations too. Both tubes test results have very low data scattering. It successfully extends the validity of conventional single-phase forced convection

heat transfer correlations to smaller tubes with inside diameter of 123  $\mu\text{m}$ .

The liquid crystal thermography method has been used very well for measuring micro tube surface temperature with uncertainties lower than  $\pm 0.4$  °C in the present study. This method can be further applied for measuring smaller tube surface temperature that the thermal shunt may be more significant by using direct contact temperature measurements methods.

#### References

- [1] Z.Y. Guo, Z.X. Li, Size effect on microscale single-phase flow and heat transfer, *Int. J. Heat Mass Transfer* 46 (2003) 149–159.
- [2] C. Camci, K. Kim, S.A. Hippensteels, A new hue capturing technique for the quantitative interpretation of liquid crystal image used in convective heat transfer studies, *J. Turbomach.* 114 (1992) 765–775.
- [3] P.T. Ireland, Z. Wang, T.V. Jones, *Measurement Techniques: Liquid Crystal Heat Transfer Measurements*, Lecture Series 1995-01, Oxford, UK, January, von Karman Institute for Fluid Dynamics, 1995.
- [4] G. Maranzana, I. Perry, D. Maillat, Mini- and micro-channels: influence of axial conduction in the walls, *Int. J. Heat Mass Transfer* 47 (2004) 3993–4004.
- [5] J.L. Hay, D.K. Hollingsworth, A comparison of trichromic systems for use in the calibration of polymer-dispersed thermochromic liquid crystals, *Exp. Therm. Fluid Sci.* 12 (1996) 1–12.
- [6] T.L. Chan, S.A. Frost, K. Jambunathan, Calibration for viewing angle effect during heat transfer measurements on a curved surface, *Int. J. Heat Mass Transfer* 44 (2001) 2209–2223.
- [7] C.-Y. Yang, J.-C. Wu, H.-T. Chien, S.-R. Lu, Friction characteristics of water, R-134a, and air in small tubes, *Microscale Thermophys. Eng.* 7 (2003) 335–348.
- [8] V. Gnielinski, New equation for heat and mass transfer in turbulent pipe and channel flow, *Int. J. Chem. Eng.* 16 (1976) 359–368.
- [9] C.-Y. Yang, S.-M. Hsu, H.-T. Chien, C.-S. Chen, Experimental investigation of liquid R-134a and water forced convection heat transfer in small circular tubes, *Trans. Aeronaut. Astronaut. Soc. Taiwan, ROC* 33 (4) (2001) 237–246.
- [10] D. Yu, R. Warrington, R. Barron, T. Ameel, An experimental and theoretical investigation of fluid flow and heat transfer in microtubes, in: *Proceedings of the Fourth ASME/JSME Joint Thermal Engineering Conference*, Maui, Hawaii, vol. 1, 1995, pp. 523–530.
- [11] T.M. Adams, S.I. Abdel-Khalik, S.M. Jeter, Z.H. Qureshi, An experimental investigation of single-phase forced convection in microchannels, *Int. J. Heat Mass Transfer* 41 (1998) 851–857.
- [12] T.-H. Yen, N. Kasagi, Y. Suzuki, Forced convective boiling heat transfer in microtubes at low mass and heat fluxes, *Int. J. Multiphase Flow* 29 (2003) 1771–1792.